EUSAR 2018; 12th European Conference on Synthetic Aperture Radar, 4-7 June 2018, Aachen Germany.
https://ieeexplore.ieee.org/document/8438011/

Imaging SAR Phenomenology of Concealed Vibrating Targets

Brandon Corbett[1], Daniel Andre[1], Darren Muff[2], Ivor Morrow[3], Mark Finnis[4]

[1] Centre for Electronic Warfare, Information and Cyber (CEWIC), Cranfield University, Shrivenham, SN6 8LA, UK
[2] Centre for Intelligence Innovation, DSTL Scientific Intelligence Team, RAF Wyton, Cambridgeshire, UK
[3] Laboratory of Electromagnetic Systems Engineering, Cranfield University, Shrivenham, SN6 8LA, UK
[4] Centre for Defence Engineering (CDE), Cranfield University, Shrivenham, SN6 8LA, UK
E-mail: b.corbett@cranfield.ac.uk

Abstract

This paper describes the novel imaging of SAR phenomena produced from vibrating targets with multipath effects. It has been established, through numerical SAR experiments, that different physical mechanisms interact to produce new artefacts. The computations demonstrated that the edges of a dielectric medium can act as a source for multipath effects to emanate from, leading to the hypothesis that SAR artefacts can arise from through-wall SAR imagery. This deduction and mechanism of origin were validated through several experimental measurements, undertaken at Cranfield University's Antennas and Ground-based SAR laboratory, yielding results that closely match those predicted.

1 Introduction

It is well known that SAR imagery can be affected by various physical phenomena, which can produce a range of artefacts within the images [1–3]. One challenging area where these phenomena are of particular interest is in the detection of running machinery within a building. Through-wall SAR has recently experienced a large increase in research activity due to the wide range of applications in both defence and civilian sectors. Surface penetrating imagery using traditional SAR methods generates image products with varying degrees of accuracy and clarity [4]. A deeper understanding of the SAR phenomena applicable to through-wall radar imagery is therefore required, leading to a clearer interpretation of the wave scattering processes in these challenging scenarios.
The intention is to advance the art and capability in SAR techniques to identify and quantify the effects produced in a SAR image from a vibrating target, which is in close proximity to a wall and provide SAR tools capable of being able to recognise running machinery within a building from a standoff location [3].

2 SAR Artefacts

The use of SAR signal processing to image a variety of different scenes and targets can cause various artefacts to appear. For example, objects moving in cross-range will produce azimuthal smearing within a SAR image [5].
The purpose of this investigation is to focus on two types of phenomena and whether they can interact to produce new artefacts.
The two phenomena (artefacts) under investigation are (i) those produced from the effect of multipath and (ii) those produced from the imaging of a vibrating target.
Multipath is being considered because when two or more targets are within close proximity *ghost* artefacts of the main target are produced down-range within the image. If a target is near to a wall, it too will experience these multipath effects and therefore produce the same type of artefacts in the SAR image.
Target vibration is also being investigated because aspects of a running machine i.e. a generator, fan, etc. can be decomposed and considered as a point scattering target with a waveform based motion, for example its position may be displaced in the form of a sinusoid wave [3].

2.1 Multipath Artefacts

Multipath artefacts are produced when a wave front of a transmitted electromagnetic wave interacts with multiple targets in the scene before being received by the antenna [1]. Multiple reflections of the wave front can also occur between targets.
Each reflection the wave front experiences, increases the path length travelled by the wave from its transmit and receive locations. The result is repeated artefacts of the target being produced within the SAR image at predictable locations downrange for each target.
Figure 1a shows a simulation image, formed using the backprojection algorithm showing the effects of multipath when two isotropic static targets are located vertically in line (perpendicular to the radar antenna) with each other, -5m and -5.5m down-range respectively.
The simulation parameters are as follows; Synthetic aperture: 2m (401 azimuthal samples), frequency range: 5-7GHz (1601 frequency samples). The simulation considers up to 7 multipath bounces. All further simulated SAR images follow these same parameters.

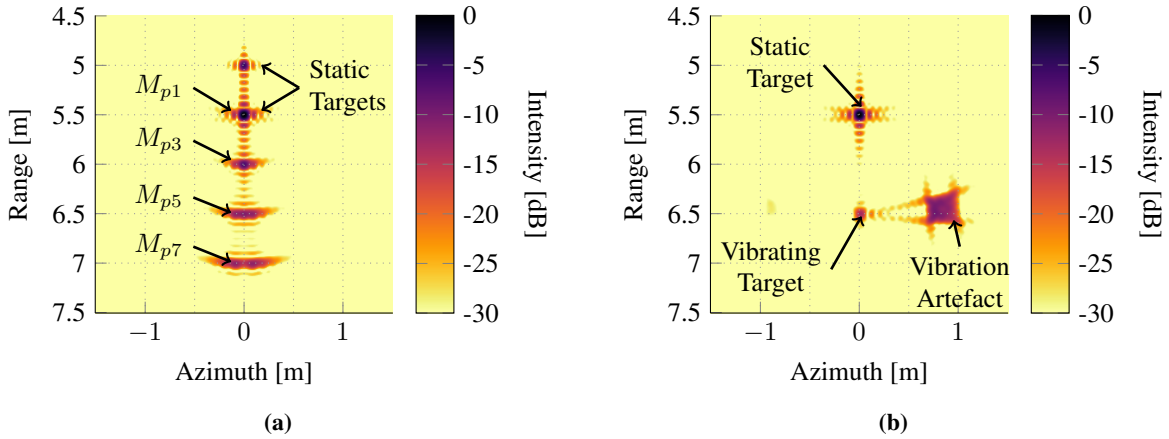

Figure 1: SAR simulation results showing individual multipath and vibration artefact scenarios. Where M_{pn} represents the n^{th} number of multipath bounces simulated. All coordinates follow the notation $[x, y, z]$m.
(a) Multipath simulation. The displacement of the multipath artefacts is equal to the 0.5m separation distance between the targets. The static and vibrating isotropic point targets are located at $[0, 5, 0]$m and $[0, 5.5, 0]$m respectively.
(b) Novel simulation of an asymmetric vibration artefact, produced when a targets motion displaces with a sawtooth waveform. The vibrating isotropic point target is located at $[0, 6, 0]$m.

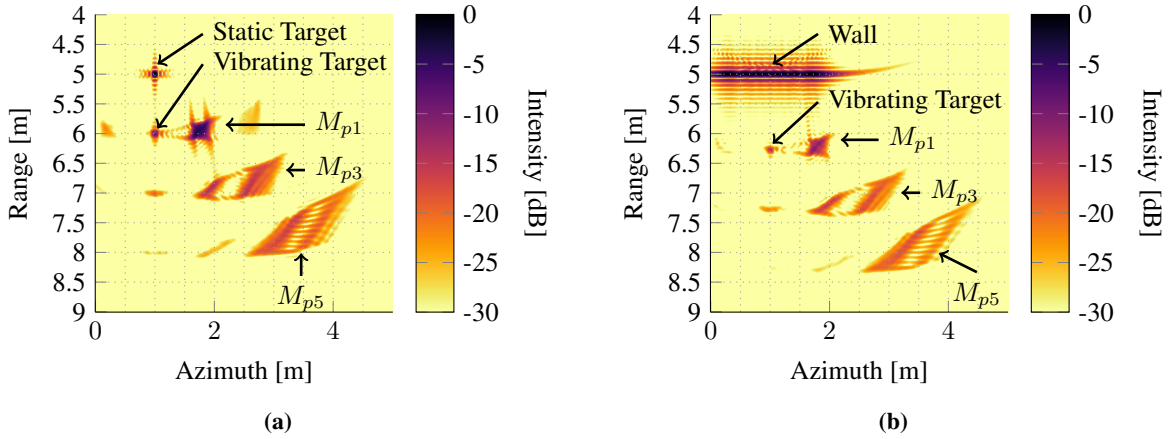

Figure 2: SAR simulation results showing combined multipath and vibration artefact scenarios. Where M_{pn} represents the n^{th} number of multipath bounces simulated. All coordinates follow the notation $[x, y, z]$m. The static/wall and vibrating isotropic point target(s) are located at $[0, 5, 0]$m and $[0, 6, 0]$m respectively.
(a) Combined multipath-vibration artefact simulation.
(b) Through-wall SAR simulation, producing combined multipath-vibration artefacts.

2.2 Vibration Artefacts

When a vibrating target is imaged using SAR signal processing, a set of a paired echoes are revealed in the image [3, 5, 6].
A detailed explanation to the physical principals that give rise to these paired-echo artefacts are presented in [2]. For example, for a target vibrating with a sinusoidal displacement in the range dimension (perpendicular to the direction of travel of the radar antennas), the effect of its displacement can be expressed as a phase modulation term that is multiplied across the phase history [2].

$$P_h\left(k_n, R_{Tn}\right) = e^{-ik_n R_{Tn}} \cdot e^{-ik_n \sin\left(2\pi f_v t_n\right)} \qquad (1)$$

Where f_v is the vibration frequency and tn is the respective time interval. The modulation term $\sin(2\pi f_v t_n)$ can be rewritten as two exponentials, equation 2, giving rise to two phase ramps where one is the complex conjugate of the other [2]. Hence, the signal response in the imaging space transforms from being a point into two separate artefacts, in opposite directions to the target location.

$$\sin\left(2\pi f_v t_n\right) = \frac{e^{i2\pi f_v t_n} - e^{-i2\pi f_v t_n}}{2i} \qquad (2)$$

During the course of this work, a novel asymmetric vibration artefact has been found. The artefact arises due to particular sawtooth target vibrations, which could occur in SAR images of partially occluded fans, say in air-conditioning units on roofs, where it is thought that these artefacts were first observed. **Figure 1b** shows a simula-

tion image of this novel asymmetric vibration artefact.

3 Combined Artefacts

Consider a vibrating target located in a scene in close approximation to other objects, it is postulated that if close enough both the multipath artefacts and vibration artefacts would combine together.

Figure 2a shows a simulation image of this where two isotropic point scatterers are located 1m apart in range. Each of the targets undergo multipath effects. The target located 5m downrange is static, while the target located at 6m downrange is vibrating with its motion following the sawtooth displacement waveform.

Developing the SAR simulator further **Figure 2b** shows the same vibrating isotropic point scatterer. However, the target located at -5m downrange has been replaced by a simulated medium (wall) of a consistent material which has the following properties; relative permittivity $\epsilon_r = 5.5$, conductivity $\sigma = 1 \times 10^2$ S/m and a wall thickness of 0.2m. These parameters were chosen as they represent the average values for a range of dielectric materials often used in building construction, e.g. concrete [3, 7].

The effects of electromagnetic wave propagation have caused the noticeable differences between Figures 2a and 2b. Firstly, wave refraction has caused a location shift to the vibrating targets image space location, the same location shift has also carried through to each of the multipath artefacts. Secondly, attenuation effects caused by the conductivity of the medium have resulted in the intensity reduction of the multipath-vibration artefacts shown [3].

4 Experimental Validation

4.1 Initial Measurement

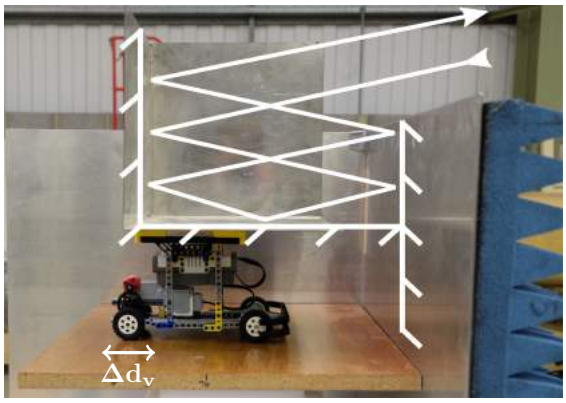

Figure 3: Experimental set-up of two metal plates used to induce multipath effects. The vibration displacement, Δd_v, of the rover is also shown.

In order to validate the numerically computed results, measurements were taken using Cranfield University's Antennas and Ground-based SAR (AGBSAR) laboratory [8]. The radar system follows a stop/start approximation, i.e. the motion of the antennas pause for each measurement. Therefore, one cannot have a continually moving target in the scene during the measurement process, hence, a moving target's motion needs to be synchronised to the radar system. The authors previously found a solution to this problem that has been validated in their previous work [3]. The synchronised moving target used is based on a Lego Mindstorms system, which communicates wirelessly over bluetooth to MATLAB and the AGBSAR radar system [3].

The first experimental set-up is shown in **Figure 3**, where the aim was to recreate the simulation results of Figure 2a. The geometry of the scene is configured so that the target under investigation is composed of two offset metal plates.

The larger of the metal plates is static in the scene and is invisible to the radar system due to the radar absorbent material (RAM) attached along its near side, facing the antennas. The second, smaller plate is a trihedral mounted on the moving target rover, orientated in parallel to the larger plate. The trihedral is in the line-of-sight of a radar antenna, shown by the augmented ray traced electromagnetic wave paths in Figure 3.

The rover displaces the trihedral towards and away from the first metal plate at a rate dependent on the vibration desired. The set-up is comparable to a fan blade moving in an air-conditioning unit.

From the experimental set-up shown in Figure 3 the following SAR image was generated, as shown in **Figure 4**. This result is in good agreement with Figure 2a and validates the mechanism proposed as the origin of multipath-vibration artefacts.

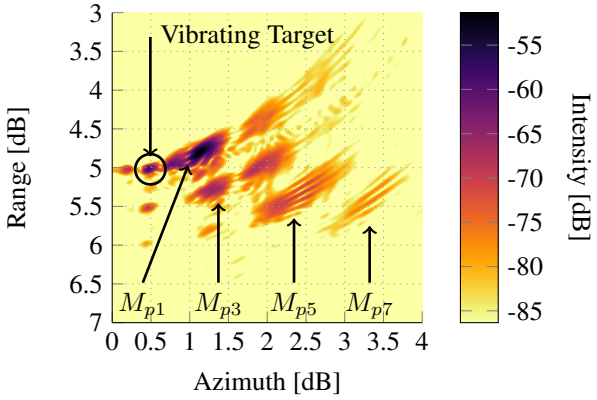

Figure 4: First measurement result of multipath-vibration artefacts. Where M_{pn} represents the n^{th} number of multipath bounces.

The measurement parameters used to collect the data of Figure 4 are as follow; Synthetic aperture: 2m (201 azimuthal samples), frequency range 4-8GHz (1601 frequency pulses), antenna height 1.8m, vibration amplitude: 10.71mm and a vibration frequency 10Hz, representing an effective antenna velocity of 2m/s.

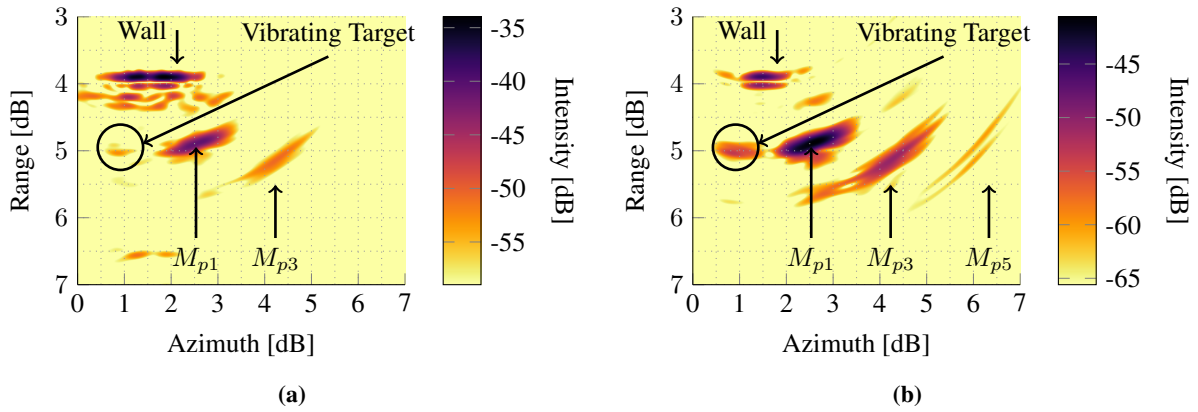

Figure 5: Measurement result of through-wall induced multipath-vibration artefacts. Both images have a 25dB dynamic range. Where M_{pn} represents the n^{th} number of multipath bounces.
(a) Non-filtered SAR measurement. Wall flash and two multipath-vibration artefacts are clearly visible.
(b) Coherent wall subtraction of Figure 5a. The flash produced by the wall has been reduced (not completely removed), while the clarity of the multipath-vibration artefacts has been increased.

4.2 Through-wall Measurement

Another experiment was set up to replicate the simulation case described in Section 3. Here the first target, i.e. the first metal plate in the experimentation set-up of Figure 3, has been replaced with a dielectric medium; a concrete masonry block wall. The wall itself is loosely built and the blocks are not secured in place by mortar/cement. **Figure 6** shows this experimental set-up.

Figure 6: Experimental set-up used for through-wall measurements.

Introducing the concrete, dielectric medium into the scene resulted in the SAR image shown in **Figure 5**. The wall is located at approximately 4m downrange of the antenna. **Figure 5a** can be compared directly to Figure 2b where the flash produced from the wall is visible in the image. The SAR measurement was collected using the following parameters; Synthetic aperture: 1.25m (125 azimuthal samples), frequency range: 2-5GHz (1601 frequency pulses), antenna height 0.86m, vibration amplitude: 21.43mm and a vibration frequency 10Hz, therefore this represents an effective antenna velocity of 2m/s.

Improvements to the SAR image of Figure 5a have been made through a coherent subtraction of a SAR dataset where the wall is the only feature in the scene. The coherent wall subtraction of **Figure 5b** results in a clearer image of the multipath-vibration artefacts.
Due to the attenuation effects of the dielectric concrete wall the artefacts have a lower intensity than previously seen in Figure 4, hence resulting in fewer multipath-vibration artefacts being visible within the given dynamic range of 35dB.

5 Conclusion

This paper has examined novel SAR imagery phenomena arising from vibrating targets and multi-path effects that result in degraded imagery. A mathematical foundation for their origin has been presented and numerical experiments of realistic scenarios simulated. Laboratory experiments replicating, as far as possible, the practical scenarios and the results of the data gathered were in good agreements with calculated. This work validates our hypothesis and the software tools and laboratory techniques will allow the investigation of more through-wall SAR phenomena and artefacts.

Acknowledgements

The authors would like to thank DSTL for partially funding this research and Cemex for supplying the concrete blocks used in the measurements. We also thank David Blacknell, Matthew Nottingham and Claire Stevenson for useful technical discussions.

References

[1] D. André, R. Hill, and C. Moate. Multipath Simulation And Removal from SAR Imagery. In Ed-

mund G. Zelnio and Frederick D. Garber, editors, *Algorithms for Synthetic Aperture Radar Imagery*, Orlando, Florida, United States, 2008. SPIE.

[2] D. Andre, D. Blacknell, D. Muff, and M. R. Nottingham. The physics of vibrating scatterers in SAR imagery. In Edmund G. Zelino and Frederick D. Garber, editors, *Aperture*, Orlando, Florida, United States, 2011. SPIE.

[3] B. Corbett, D. André, and M. Finnis. Through-Wall Detection and Imaging of a Vibrating Target Using Synthetic Aperture Radar. *IET Electronics Letters*, 53(15):991–995, 2017.

[4] M. Amin and F. Ahmad. Through-the-Wall Radar Imaging: Theory and Applications. *Academic Press Library in Signal Processing*, 2:857–909, 2014.

[5] Walter G. Carrara, Ron S. Goodman, and Ronald M. Majewski. *Spotlight Synthetic Aperture Radar, Signal Processing Algorithms*. Artech House, INC, first edition, 1995.

[6] M. Ruegg, E. Meier, and D. Nuesch. Constant Motion, Acceleration, Vibration, and Rotation of Objects in SAR Data. In *SAR Image Analysis, Modeling, and Techniques VII*, volume 5980, pages 598005–598005–12. SPIE, 2005.

[7] David Daniels. *Ground Penetrating Radar*. Institution of Engineering and Technology, second edition, 2004.

[8] D. André, K. Morrison, D. Blacknell, D. Muff, M. Nottingham, and C. Stevenson. Very high resolution Coherent Change Detection. *Radar Conference (RadarCon), 2015 IEEE*, pages 634–639, 2015.